Journal of Engg. Research ICAPIE Special Issue pp. 72-81 DOI:10.36909/jer.ICAPIE.15071

Effect of Cylindrical Shaped Material Perturbation on Resonance of Dielectric Resonator Antenna

Neetu Sehrawat*, Anshul Agarwal** and B.K. Kanaujia***

*Department of Electronics & communication Engineering, National Institute of Technology, Delhi, 110040, MSIT, Delhi, 110058, India.
**Department of Electrical & Electronics Engineering, National Institute of Technology, Delhi, 110040, India
***School of Computational & Integrative Sciences, Jawaharlal Nehru University, Delhi, 110067, India
*Corresponding Author: neetu.aries2006@gmail.com

ABSTRACT

The paper presents a concept of cylindrical shaped material perturbation in rectangular dielectric resonator antenna (RDRA) which can be used for gain and bandwidth enhancement over original DRA. Material perturbation of cylindrical shape in two orthogonal directions will result in change of resonance of isotropic rectangular dielectric resonator antenna. The Effect of change of radius of cylinder for different dielectric materials is investigated. The proposed RDRA with centered cylindrical shape perturbation (PRDRA_CC) is analyzed theoretically using perturbation theory and simulated on 3D EM simulator HFSS. Theoretical and simulated results are compared and good agreement between two is obtained. Material perturbation provide wide tuning range, improved degree of freedom and hence more flexibility in designing antenna for given frequency range of application. Further, material perturbation and wall perturbation can be combined for obtaining polarization diversity in DRAs.

Keywords: Anisotropic material; mylindrical shaped material perturbation; Rectangular dielectric resonator antenna; Resonant frequency.

INTRODUCTION

Dielectric Resonator Antennas (DRAs) are preferred in linear as well as circularly polarized systems due to its low losses, ease of excitation, light weight, higher gain and radiation efficiency. Dual band dual port three dimensional circularly polarized MIMO DRA (Singhwal et al., 2020) are widely used for wireless communication applications. Much work has been done on rectangular dielectric Resonator Antennas (DRAs) because of greater design flexibility and less cross polarization over other shapes of DRA (Petosa, 2007, Leung et al., 2012, Abedian et al., 2018 &Fakhte et al. 2019).

Analysis of two layer inhomogeneous stacked rectangular (Maity et al., 2017 & Petosa et al., 2000), cylindrical (Ghosal et al., 2020) and triangular (Maity et al. 2016) dras are recently done for prediction of resonant frequency. Frequency of operation of antenna is great area of research for designing application specific antennas. Numerical methods based on different techniques have been reported in literature (Glisson et al., 1983, Kishkk et al., 1993, &Mongia et al., 1997) for calculating the resonant frequency of operation of antenna. Perturbation approach (Peng et al., 2014) for basic RDRA for calculation of dominant mode resonant frequency and q factor is given. Analysis of RDRA with rectangular shaped perturbation (Sehrawat et al., 2019) is reported and higher accuracy of perturbation theory for analysis of stacked and layered RDRA over other reported methods is shown.

This paper is extension of perturbation theory for cylindrical shaped material perturbation which is previously applied for accurate calculation of resonant frequency of Rectangular shaped perturbation in RDRA (Sehrawat et al., 2019). Recently DRA (Varshney et al., 2016) with anisotropic material has been analyzed using concept of effective homogeneity tensor (Fakhte et al., 2016) and equivalence theorem (Fakhte et al., 2017) for gain and boresight directivity improvement. Perturbation makes RDRA anisotropic structure and RDRA of higher dielectric constant with centered cylinder of low dielectric constant will lead to boresight gain enhancement. Anisotropic crystals are very costly,

make them less practical for use. Theory can be extended for other shapes of perturbation like triangular. Triangular DRA are lower in size than RDRA made of same material and same size, operating at same frequency.

THEORY

A homogeneous Rectangular Dielectric resonator antenna is excited in dominant mode using probe feed (Sehrawat et al., 2019. Fig. 1) and subjected to cylindrical shaped material perturbation. The Rectangular DRA has dimensions a, b, d along x, y and z direction respectively and is made of material having Dielectric constant of . The RDRA with centered cylinder is shown in Fig. 1. The change in resonant frequency of the dominant mode due to cylindrical shaped material perturbation is presented here. Perturbation theory is used for calculating the resonant frequency of perturbed RDRA.The electric and magnetic field components, resonant frequency and stored energy of original RDRA must be known for applying perturbation theory. The field components of homogeneous RDRA Equation, derived in (Sehrawat et al., 2019, Equation 1-6) and expressed in terms of arbitrary constant A and wave numbers along x, y and z direction. Transcendental equation for resonant frequency ( ) calculation are given by Equation 1-3. Perturbation approach for isolated RDRA is given by (Sehrawat et al., 2019 Equation (11,12)]. The symbols and terms used in paper are given by Table 1.

$$k_x = \frac{\pi}{a}, \quad k_y = \frac{\pi}{b} \tag{1}$$

$$k_x{}^2 + k_y{}^2 + k_z{}^2 = \varepsilon_r k_0{}^2 \tag{2}$$

$$k_z \tan\left(k_z \frac{d}{2}\right) = \sqrt{(\varepsilon_r - 1)k_0{}^2 - k_z{}^2} \tag{3}$$

Perturbation approach can be expressed in terms of stored energy of RDRA having resonant frequency f_r and relative permittivity $\sum_r$:

$$\frac{f_{rp} - f_r}{f_r} = \frac{\Delta w_m - \Delta w_s}{w_m + w_s} = -\frac{\iiint \Delta\varepsilon E_p . E_0^* d\tau}{2 \iiint \varepsilon_r \left| E_0 \right|^2 d\tau} \tag{4}$$

$$W_s + W_m = \frac{\epsilon_0 \varepsilon_r A^2 abd}{16}\left[k_x{}^2 + k_y{}^2\right][1 + \sin c(k_z d)] \tag{5}$$

$$\Delta w_m - \Delta w_s = \frac{\epsilon_0 A^2 d}{16 k_0^2}\left[k_z{}^2 - k_0{}^2\right]\left[\frac{k_x{}^2 b}{\sqrt{(\varepsilon_r - 1)^2 k_0{}^2 - k_x{}^2}} + \frac{k_y{}^2 a}{\sqrt{(\varepsilon_r - 1)^2 k_0{}^2 - k_y{}^2}}\right] \tag{6}$$

$$f_{rp} = f_r + df_r \tag{7}$$

$$df_r = f_r \times \frac{\left(\frac{k_z}{k_0}\right)^2 - 1}{\varepsilon_r ab} \times \frac{1}{1 + \sin c(k_z d)} \times \frac{\frac{k_x{}^2 b}{\sqrt{(\varepsilon_r - 1)^2 k_0{}^2 - k_x{}^2}} + \frac{k_y{}^2 a}{\sqrt{(\varepsilon_r - 1)^2 k_0{}^2 - k_y{}^2}}}{k_x{}^2 + k_y{}^2} \tag{8}$$

Where $\Delta w_m - \Delta w_s$ = Change in stored energy due to perturbation , $W_s + W_m$ = total stored energy of original RDRA, , $\Delta\varepsilon = \varepsilon_p - \varepsilon_r$ E_0 =Electric Field of original RDRA, E_p =Electric Field of perturbed region of RDRA.

Perturbed rectangular DRA with centered cylinder placed vertically (PRDRA_CPV)

When RDRA excited in TE^{z}_{111} mode using probe feed at position $(\frac{a}{2},0,0)$, cylinder of radius R can be placed vertically along y-axis as shown in Fig. 1(a) Height of cylinder (h) is equal to dimension of RDRA along y axis (b) for this case. Dielectric discontinuity is created at outer boundary of cylinder due to perturbation. The continuity of tangential component at the discontinuity is maintained when electric field intensity in perturbed cylindrical region (E_p) is equal to electric field intensity in original RDRA (E_o)

$$E_0 = E_p \tag{9}$$

Substitute equation (9) into equation (4)

$$\frac{f_{CPVY} - f_{rp}}{f_{rp}} = -\left(\frac{\varepsilon_p}{\varepsilon_r} - 1\right)\left(\frac{b^2}{a^2 + b^2}\right)\left(\frac{\pi R^2}{ad}\right) \tag{10}$$

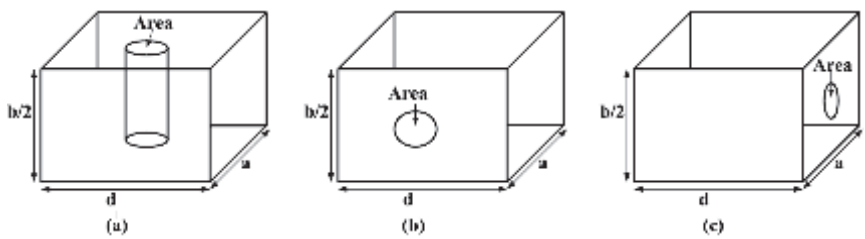

Figure 1. Perturbed RDRA excited in mode with (a) centred cylinder placed along y axis , (b) centred cylinder placed along x axis, (c) centred cylinder placed along z axis

Perturbed rectangular DRA with centered cylinder placed horizontally (PRDRA_CPH)

The cylinder of radius R can be placed horizontally along x and z axis when RDRA is excited in mode as shown in Fig. 1(b) and 1(c) Height of cylinder h=a when placed horizontally along x axis and h=d when placed horizontally along z axis. Normal component of Electric Flux Densitywill be continuous at dielectric discontinuity when field intensity in perturbed and original region satisfy the following condition.

$$E_p = 2\varepsilon_r E_0/(\varepsilon_p + \varepsilon_r) \tag{11}$$

Substituting equation (11) into equation (4)

$$\frac{f_{CPHX} - f_{rp}}{f_{rp}} = -2\left(\frac{\varepsilon_p - \varepsilon_r}{\varepsilon_p + \varepsilon_r}\right)\left(\frac{b^2}{a^2 + b^2}\right)\left(\frac{\pi R^2}{bd}\right) \tag{12}$$

$$\frac{f_{CPHZ} - f_{rp}}{f_{rp}} = -2\left(\frac{\varepsilon_p - \varepsilon_r}{\varepsilon_p + \varepsilon_r}\right)\left(\frac{b^2}{a^2 + b^2}\right)\left(\frac{\pi R^2}{ab}\right) \tag{13}$$

Hence, resonant frequency of PRDRA excited in can be calculated from Equation (10),(12) and (13). Fig. 2(a) and 2(b) shows the graphical representation of perturbation approach for mode of PRDRA in terms of normalized frequency. These graphs are drawn on MATLAB using equations (10), (12) and (13). Formulas for are given in Table 2.

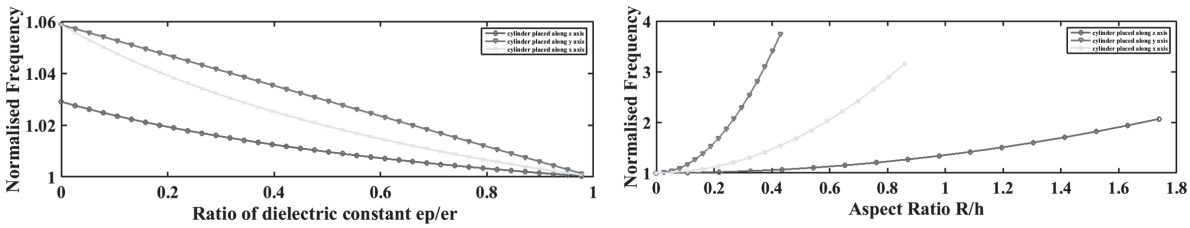

Figure 2. Normalised frequency (a) when Radius of cylinder(R) is constant and relative dielectric constant of cylinder is varied (b) Radius of cylinder(R) is varied and relative dielectric constant of cylinder is kept constant

Table 1. The symbols and terms used in the paper

Symbol used for RDRA without perturbation

a, b, d	Dimensions of RDRA along x, y and z axis respectively.
ε_r	Dielectric constant of RDRA
K_x, K_y, K_z	Wave number along x, y and z directions respectively.
f_{rp}	Resonant frequency of RDRA using perturbation method
f_{HFSS}	Simulated Resonant frequency of RDRA

Symbols used RDRA with cylindrical shaped material perturbation

R	Radius of cylinder, R=r1=1mm & R=r2=2mm
ε_p	Dielectric constant of cylinder, $\varepsilon_p = \varepsilon_0, \varepsilon_1, \varepsilon_2, \varepsilon_3 \& \varepsilon_4$ where $\varepsilon_0 = 1$, ε_1=10.2, ε_2=20, ε_3=30, ε_4=40
f_{CPHX}	Resonant frequency of RDRA when cylinder is placed along X axis
f_{HFSS_X}	Simulated resonant frequency of RDRA when cylinder is placed along X axis
f_{CPVY}	Resonant frequency of RDRA when cylinder placed along Y axis
f_{HFSS_Y}	Simulated resonant frequency of RDRA when cylinder placed along Y axis
f_{CPHZ}	Resonant frequency of RDRA when cylinder placed along Z axis
f_{HFSS_Z}	Simulated resonant frequency of RDRA when cylinder placed along Z axis

Table 2. Perturbation approach for resonant frequency of TE^{z}_{111} TE^{y}_{111} ,TE^{x}_{111} , mode of RDRA

Mode	Direction and placement of Cylinder of Radius R	Perturbation approach for RDRA having Cylindrical Shaped Perturbation
TE^{z}_{111}	Horizontally along X axis	$\frac{f_{CPHX}-f_{rp}}{f_{rp}}=-2\left(\frac{\varepsilon_p-\varepsilon_r}{\varepsilon_p+\varepsilon_r}\right)\left(\frac{b^2}{a^2+b^2}\right)\left(\frac{\pi R^2}{bd}\right)$
	Horizontally along Z axis	$\frac{f_{CPHZ}-f_{rp}}{f_{rp}}=-2\left(\frac{\varepsilon_p-\varepsilon_r}{\varepsilon_p+\varepsilon_r}\right)\left(\frac{b^2}{a^2+b^2}\right)\left(\frac{\pi R^2}{ab}\right)$
	Vertically along Y axis	$\frac{f_{CPVY}-f_{rp}}{f_{rp}}=-\left(\frac{\varepsilon_p}{\varepsilon_r}-1\right)\left(\frac{b^2}{a^2+b^2}\right)\left(\frac{\pi R^2}{ad}\right)$
TE^{y}_{111}	Horizontally along X axis	$\frac{f_{CPHX}-f_{rp}}{f_{rp}}=-2\left(\frac{\varepsilon_p-\varepsilon_r}{\varepsilon_p+\varepsilon_r}\right)\left(\frac{d^2}{a^2+d^2}\right)\left(\frac{\pi R^2}{bd}\right)$
	Horizontally along Y axis	$\frac{f_{CPHY}-f_{rp}}{f_{rp}}=-2\left(\frac{\varepsilon_p-\varepsilon_r}{\varepsilon_p+\varepsilon_r}\right)\left(\frac{d^2}{a^2+d^2}\right)\left(\frac{\pi R^2}{ad}\right)$
	Vertically along Z axis	$\frac{f_{CPVZ}-f_{rp}}{f_{rp}}=-\left(\frac{\varepsilon_p}{\varepsilon_r}-1\right)\left(\frac{d^2}{a^2+d^2}\right)\left(\frac{\pi R^2}{ab}\right)$
TE^{x}_{111}	Horizontally along X axis	$\frac{f_{CPHX}-f_{rp}}{f_{rp}}=-2\left(\frac{\varepsilon_p-\varepsilon_r}{\varepsilon_p+\varepsilon_r}\right)\left(\frac{b^2}{b^2+d^2}\right)\left(\frac{\pi R^2}{bd}\right)$
	Horizontally along Z axis	$\frac{f_{CPHZ}-f_{rp}}{f_{rp}}=-2\left(\frac{\varepsilon_p-\varepsilon_r}{\varepsilon_p+\varepsilon_r}\right)\left(\frac{b^2}{b^2+d^2}\right)\left(\frac{\pi R^2}{ab}\right)$
	Vertically along Y axis	$\frac{f_{CPVY}-f_{rp}}{f_{rp}}=-\left(\frac{\varepsilon_p}{\varepsilon_r}-1\right)\left(\frac{b^2}{b^2+d^2}\right)\left(\frac{\pi R^2}{ad}\right)$

Table 3. TE^{z}_{111} mode Resonant frequencies of PRDRA with centered dielectric cylindrical placed horizontally along X & Z axis and placed vertically along Y axis.

Radius of cylinder	Dielectric Constant		Calculated Resonant frequency for different orientation of cylinder			Simulated Resonant frequency for different orientation of cylinder		
R(mm)	ε_p	ε_r	f_{CPHX} (GHz)	f_{CPVY} (GHz)	f_{CPHZ} (GHz)	f_{HFSS_X} (GHz)	f_{HFSS_Y} (GHz)	f_{HFSS_Z} (GHz)
1	1	37.84	4.5084	4.5147	4.3882	4.443	4.3356	4.255
1	10.2	37.84	4.4149	4.4538	4.342	4.3356	4.255	4.2282
1	20	37.84	4.348	4.3889	4.3089	4.2819	4.2282	4.2013
1	30	37.84	4.2997	4.3226	4.285	4.2282	4.2013	4.2013
1	40	37.84	4.2638	4.2564	4.2673	4.1745	4.1745	4.1745
2	1	37.84	5.2216	5.2467	4.7405	5.2483	5.0336	4.4161
2	10.2	37.84	4.8475	5.003	4.5557	4.8725	4.6309	4.3356
2	20	37.84	4.5799	4.7434	4.4235	4.5503	4.3893	4.2819
2	30	37.84	4.3866	4.4784	4.328	4.3087	4.255	4.2282
2	40	37.84	4.2429	4.2135	4.257	4.1477	4.1477	4.1745

Table 4. comparison and % error of mode Resonant frequencies of PRDRA with dielectric cylindrical placed horizontally along X & Z axis and placed vertically along Y axis.

Radius of cylinder	**Dielectric Constant**		**% Error between Calculated and Simulated Resonant frequency for different orientation of cylinder**		
R(mm)	ε_p	ε_r	$\Delta f_{CPHX}=\frac{f_{CPHX}-f_{HFSS\ X}}{f_{HFSS\ X}}$	$\Delta f_{CPVY}=\frac{f_{CPVY}-f_{HFSS\ Y}}{f_{HFSS\ Y}}$	$\Delta f_{CPHZ}=\frac{f_{CPHZ}-f_{HFSS\ Z}}{f_{HFSS\ Z}}$
1	1	37.84	1.47%	4.13%	3.13%
1	10.2	37.84	1.83%	4.67%	2.69%
1	20	37.84	1.54%	3.80%	2.56%
1	30	37.84	1.69%	2.89%	1.99%
1	40	37.84	2.14%	1.96%	2.22%
2	1	37.84	-0.51%	4.23%	7.35%
2	10.2	37.84	-0.51%	8.04%	5.08%
2	20	37.84	0.65%	8.07%	3.31%
2	30	37.84	1.81%	5.25%	2.36%
2	40	37.84	2.30%	1.59%	1.98%

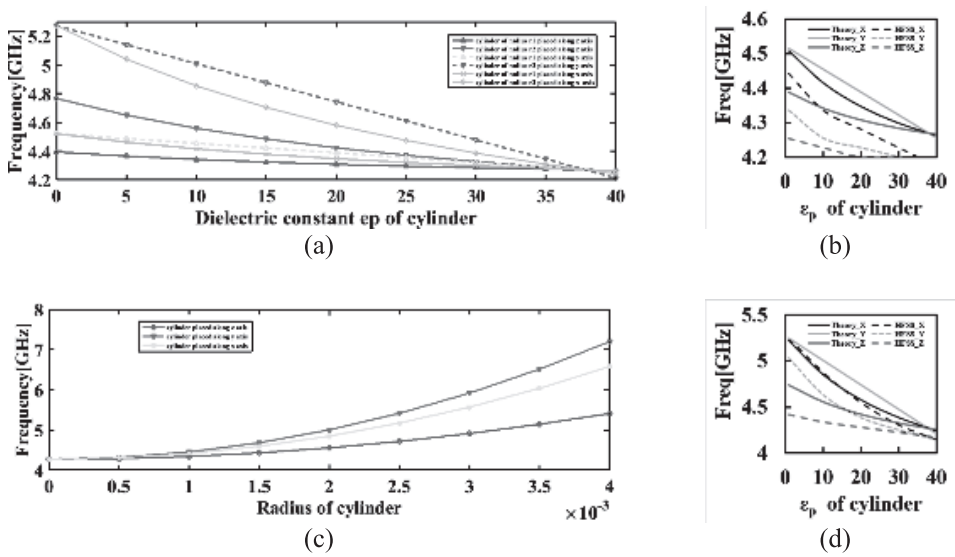

Figure 3. comparison of theoretical Resonant frequencies of PRDRA w.r.t (a) dielectric constant of cylinder (r_1 =1mm, r_2 =2mm) (b)radius of cylinder (ε_p = 10.2). (c) simulated resonant frequencies for radius R= r_1 =1mm (d) simulated resonant frequencies for radius R= r_2=2mm

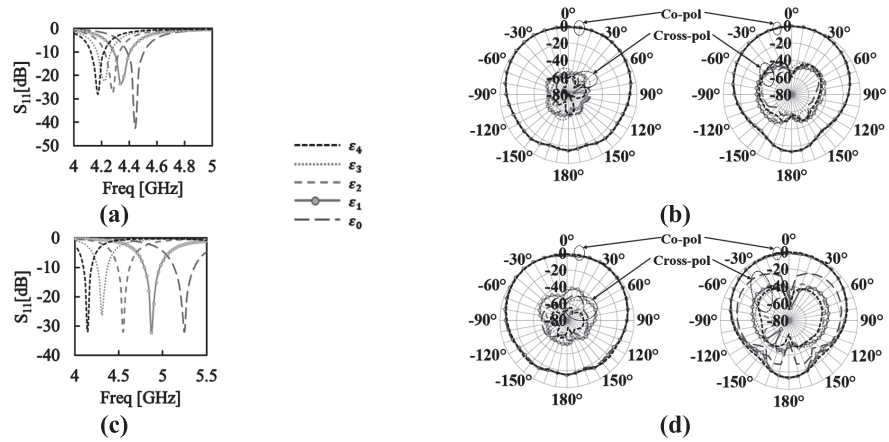

Figure 4. Simulated (a), (c) S11 and (b), (d) radiation pattern of PRDRA_CPH when cylinder of radius r_1 and r_2 respectively placed horizontally along x axis

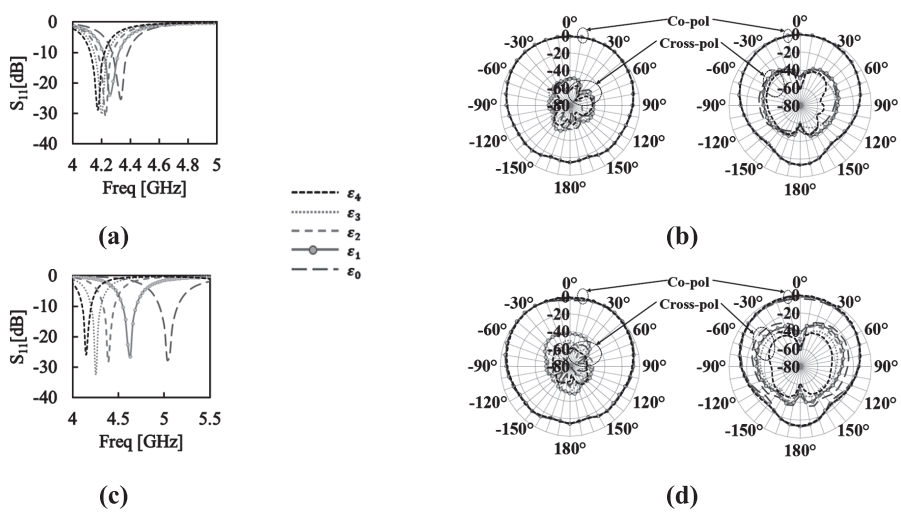

Figure 5. Simulated (a), (c) S11 and (b), (d) radiation pattern of PRDRA_CPV when cylinder of radius r_1 and r_2 respectively placed vertically along y axis

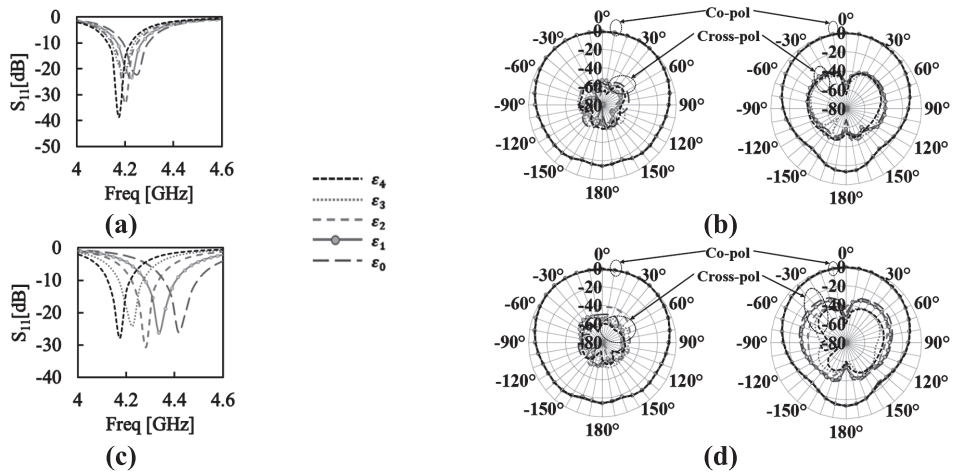

Figure 6. Simulated (a), (c) S11 and (b), (d) radiation pattern of PRDRA_CPH when cylinder of radius r_1 and r_2 respectively placed horizontally along z axis

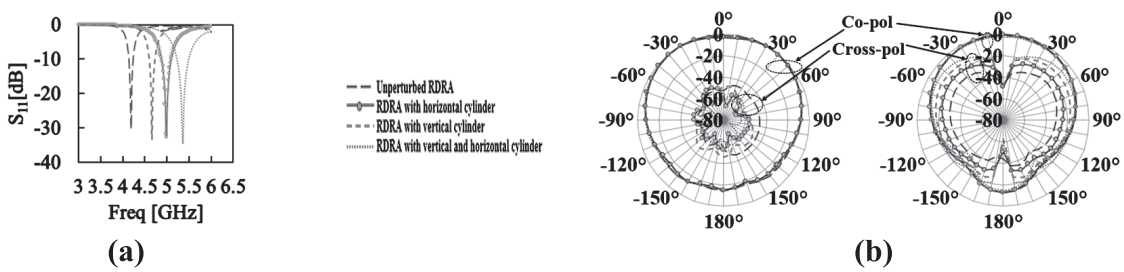

Figure 7. comparison of simulated result of RDRA and PRDRA_CH and PRDRA_CV (a) S_{11} (b) radiation pattern.

RESULTS AND DISCUSSION

Purpose of using perturbation theory for analysis of RDRA is its accuracy over the conventional dielectric waveguide model method. For validation of our theory, number of simulations are performed using high frequency structure simulator (HFSS).RDRA (9.31 x 18.62 x 4.6) is excited in dominant mode using probe feed (4.655,0,0). Resonant frequency (for the given RDRA calculated from perturbation theory is 4.2707GHz. Comparison of theoretical and simulated resonant frequency (=4.1879 GHz) is shown in (Sehrawat et al., 2019, Table 1, Fig 6a).

The given RDRA is subjected to cylindrical shaped material perturbation. The resonant of Perturbed RDRA is calculated using Equation (10), (12), (13). Height of cylinder h is equal to a, b, d when cylinder is placed along x, y, and z axis respectively. For increasing the flexibility in antenna designing either the radius of cylinder (R) or its dielectric constant ( ) can be varied for particular orientation of centered cylinder. Three factors which affect the resonant frequency of perturbed RDRA are: (I)Radius of cylinder (R) , (II) Dielectric constant of cylinder (& (III) Direction of placed of cylinder (Horizontal or Vertical). Effect of these factors is shown graphically in Fig. 2(a) and Fig. 2(b). In Fig. 2(a), variation of normalized frequency w.r.t ratio of dielectric constant (shows that as the ratio (increases the resonant frequency of PRDRA decreases for fixed radius of cylinder. In Fig. 2(b), variation of normalized frequency w.r.t aspect ratio (shows that as the ratio (increases the resonant frequency of PRDRA also increases. Effect of these factors are verified using simulation.

Case: (I) Effect of Dielectric constant of cylinder: When dielectric constant (ε_p) is increased from ε_0 to ε_4, frequency decreases from 4.5084GHz to 4.2638GHz for radius R=r_1 and 4.7405GHz to 4.2570GHz when radius R= r_2 =2mm. Frequency decreases from 4.5147GHz to 4.2564GHz for radius R=r_1 =1mm and decreases from 5.2467GHz to 4.2135GHz for radius R= r_2=2mm. Frequency decreases from 4.3882GHz to 4.2673GHz for radius R= r_1 =1mm and decreases from 4.7405GHz to 4.2570GHz for radius R=r_2 =2mm.

For fixed value of dielectric constant (ε_p)=10.2 and radius of cylinder R is increased from 0 to 2mm, frequency increases from 4.2707GHz to 4.5557GHz.

Case:(II) Effect of radius of cylinder:For fixed value of dielectric constant (ε_p)=10.2 when radius of cylinder R is increased from 0 to 2mm, frequency f_{CPHX} & f_{CPHZ} increases to 4.5557GHz, f_{CPVY} increases to 5.003GHz from 4.2707 GHz.

Case I and II are in agreement with the proposed theory normalized frequency graph shown in Figure 2. Comparison of data obtained from theory and simulation is shown in Table 3 and Table 4. Comparison of theoretical results for all three cases is shown in Figure 3(a) & 3(b). Graphical representation of comparison of resonant frequency obtained from (THEORY_X, THEORY _Y, THEORY_Z) and simulation (HFSS_X, HFSS_Y, HFSS_Z) is shown in Figure 3(c) and 3(c). Figure 3(b) and 3(d) show that theoretical results are in very good agreement with simulated results.

Comparison of RDRA, PRDRA when cylinder placed horizontally and vertically is shown in Figure 7. Maximum change in resonant frequency as compared to unperturbed RDRA is observed when material perturbation is made in both directions. Hence, For fixed radius and fixed dielectric constant of cylinder, $f_{rp} < f_{CPH} < f_{CPV} < f_{CPHV}$.

RDRA with material perturbation will result in inhomogeneous structure, changes the effective dielectric constant and hence the antenna characteristics. The perturbation approach can be utilized for designing desirable antenna by identification of nearby mode. This concept of material perturbation can be used to make uniaxial or biaxial anisotropic material which further can be used for boresight gain enhancement of isotropic RDRA. Theory can be extended for perturbation of other shape.

CONCLUSION

In this paper, the concept of rectangular cavity with centered dielectric is applied to analyze RDRA having centered dielectric cylinder. Perturbed dielectric cylinder can be placed along any axis resulting in anisotropic RDRA. Depending on mode of excitation, placement of cylinder will be horizontal or vertical. Quasi-static approximation for dielectric cylinder and boundary conditions are applied together at dielectric discontinuity for analysis of dominantmode of RDRA. A simple equation, in terms of ratio of change in stored electric and magnetic energy in perturbed RDRA to total stored energy in unperturbed RDRA, is given to predict the resonant frequency of RDRA with dielectric cylinder. Theoretical and simulated frequencies are compared and calculated percentage error is within the acceptable range. Proposed analysis using perturbation theory can be used to calculate resonant frequency of perturbed RDRA for arbitrary radius and material of centered cylinder. Flexibility in DR antenna designing isincreased due to addition of two more parameters which is radius and dielectric constant of cylinder over isotropic RDRA. Concept of material perturbation can be extended for any othershapes such as spherical, triangular etc and can be combined with wall perturbation for introducing polarization diversities.

REFERENCES

Singhwal, S.S., Kanaujia, B.K., Singh, A., Kishor, J. & Matekovits, L. 2020. Dual-band circularly polarized MIMO DRA for sub-6 GHz applications. Internatioal journal of RF and Mirowave computer aided engineering. 30(10): 1–12.

Petosa, A. 2007. Dielectric Resonator Antenna Handbook Artech House Antennas and Propagation Library.

Leung, K.W., Lim, E.H. & Fang, X.S., 2012. Dielectric resonator antennas: From the basic to the aesthetic. Proceedings of the IEEE 100 (7): 2181–93.

Abedian, M. et al. 2018. Wideband rectangular dielectric resonator antenna for low-profile applications. IET microwave, antennas and propagation. 12(1): 115–119.

Fakhte, S., Matekovits, L. & Aryanian, I. 2019. Rectangular Dielectric Resonator Antenna with Corrugated Walls. IEEE Access 7: 3422–29.

Maity, S. & Gupta, B. 2017. Theory and experiments on horizontally inhomogeneous Rectangular Dielectric Resonator Antenna. AEUE - International Journal of Electronics and Communications. 76: 158–165.

Petosa, A., Simons, N. R. Siushansian, Ittipiboon, A. & Cuhaci, M. 2000. Design and Analysis of Multisegment Dielectric Resonator Antennas. 48(5): 738–742.

Ghosal, R., Maity, S., gupta, B. & Majumder, A.2020. Analytical prediction of Resonant Frequency of annular Stacked Dielectric Resonator Antenna. Internatioal journal of RF and Mirowave computer aided engineering. 30(8): 1–17.

Maity, S. & Gupta, B. 2016. Experimental Investigations on Wideband Triangular Dielectric Resonator Antenna. IEEE transactions on antenna and propagation. 64(12): 5483-5486.

Glisson, A.W., Kajfez, D. & James, J. 1983. Evaluation of Modes in Dielectric Resonators Using a Surface Integral Equation Formulation. IEEE transaction on microwave theory and techniques. 31(12): 1023-1029.

Kishk, A.A., Zunoubi, M.R., & Kajfez, D. 1993. A Numerical Study of a Dielectric Disk Antenna Above Grounded Dielectric Substrate. IEEE transactions on antennas and propagatiion. 41(6): 813–821.

Mongia, R.K. & Ittipiboon, A. 1997. Theoretical and experimental investigations onrectangular dielectric resonator antennas. IEEE Transactions on Antennas and Propagation.45(9): 1348–56.

Peng, Z., Hwang, J. & Andriese, M. 2014. Maximum Sample Volume for Permittivity Measurements by Cavity Perturbation Technique. IEEE transaction on instrumentation and measurement. 63(2): 450–455.

Sehrawat, N., Kanaujia, B.K., & Agarwal, A. 2019. Calculation of the resonant frequency of a rectangular dielectric resonator antenna using perturbation theory. Journal of Computational Electronics. 18(1): 211-221.

Varshney, G., Pandey, V.S., & Yaduvanshi, R.S. 2016. Wide band circularly polarized dielectric stair shaped slot excitation. . IEEE transactions on antennas and propagation 65(3): 1680-1683.

Fakhte, S. & Oraizi, H. 2016. Compact Uniaxial Anisotropic Dielectric Resonator Antennawith Enhanced Gain. Electronics Letter. 52(19): 157-1580.

Fakhte, S., Oraizi, H. & Matekovits, L. 2017. High gain rectangular antenna using uniaxial material at fundamental mode. IEEE Transactions on Antennas and propagation. 65(1): 342-347.